

# LAND COVER CLASSIFICATION USING AIRBORNE LASER SCANNING DATA AND PHOTOGRAPHS

P. Tymkow, A. Borkowski

Department of Geodesy and Photogrammetry Wrocław University of Environmental and Life Sciences  
Wrocław, C.K. Norwida 25/27, POLAND (tymkow, borkowski)@kgf.ar.wroc.pl

**KEY WORDS:** Airborne remote sensing, Surface roughness coefficient, Image understanding, Data Integration, Flood management, Land Cover

## ABSTRACT:

The main purpose of this project was to investigate the possibility of using airborne laser scanning data as a source of information for supervised land cover classification of Widawa River valley. The project was done for the need of hydrodynamic modeling of flood. Laser scanning data was used both as a sole and supplementary source of information about land cover. The second approach was based on non-metric aerial photographs taken during laser data acquisition. Aerial photographs were directly included in vector classification as RGB channels. They were also applied in GLCM texture features calculation. On the strength of laser scanning data and photographic features, large numbers of experiments were performed to find the best combination of data set and classification methods. In order to quantify the quality of the results, a confusion matrix was created for each case. As a quality parameters kappa coefficient, producer and user accuracy were proposed. These experiments demonstrated that scanning data, as the only source of information, is insufficient for land cover classification. However, by including altitudes and RGB and texture features in vector classification results improve. The replacement of differential model estimated on the basis of DSM and DTM with height variance gives comparable results. The inclusion of intensity image in the feature vector does not reduce false classification rate in a significant way. However this information is useful for water detection even if it is invisible on aerial photographs. The best results are obtained by an artificial neural network classifier.

## 1. INTRODUCTION

### 1.1 Background

Airborne laser scanning data (point cloud) is generally applied in digital terrain models (DTMs) and digital surface models (DSMs) generation. Nowadays, it is also used for geoinformation modeling (trees, buildings, etc.). However, the direct and indirect information about terrain surface and land use included in laser scanning data sets also supports the automatic classification of land cover. On the other hand, categorization of aerial and satellite image contents using the spectral analysis or other features like textures can be insufficient in some cases. Classification of land cover, which takes into consideration vegetation density below the treetop level in the forest area, can be an example of such problem. Because the laser beam can penetrate even dense vegetation, it gives some information on features which are invisible on satellite images or photogrammetric photographs. In addition to detailed information on geometry, laser intensity image is recorded, which characterizes the reflectance of the Earth's surface. This feature also includes some information on land cover and can be used in classification process but its usefulness for afforested areas is still discussed in literature. Original intensity data has to be calibrated and interpolated into intensity image before using. In the project only coarse calibration was performed. It was based on a distance between sensor and scanning point on the reflective surface. Because the large part of the study area was wooded, precise calibration on satisfying level was not possible.

Over the last years, flooding has become a huge hazard. The flood of the Odra river in 1997 was the biggest environmental catastrophe in Poland in the XX century. Flood protection and prediction are becoming very important nowadays. Hydrodynamic models are one of the most important tools for this studies. These models require hydrological and geospatial data. The terrain model quality and land cover characteristics determine the hydrodynamic model correctness. Modern 2D and 3D hydrodynamic models use Digital Terrain Model (DTM) for topography description and land cover classification maps as the source of information on surface roughness.

### 1.2 Previous Work

Utility of land cover classification was a subject of previous investigations. Charaniya, Manduchi and Lodha (Charaniya et al., 2004) used aerial LiDAR data to examine parametric classification of such land cover classes as road, grass, buildings and trees. They used normalized height of objects from DTM models, height texture feature computed as a difference between maximum and minimum height values in a window, difference of first and last return signal, intensity image and luminance obtained from gray-scale aerial photographs. As a classifier, they used Maximum likelihood method based on mixture of Gaussian models for training data modeling. Model parameters and the posterior probabilities were estimated using Expectation - Maximization (EM) algorithm. Outcomes of the research were satisfactory. Authors have checked different combinations of the feature vector. Finally, they recognized the height feature as very important one for terrain classification. Moreover, inclusion of luminance and intensity improves recognition accuracy. Katzenbeisser (Katzenbeisser, 2003) conducted experiments to prove the utility of reflection intensity in the forest area analysis. His investigations contains a detailed description of laser impulses registration for the vegetation area. As an example, he studied intensity reduction of a single impulse reflection transmitted to the wooden area. Song (Song et al., 2002) conducted research works whose aim was to determine land use classes on the basis of information on reflection intensity. Results were not satisfactory for the classification of vegetated areas. Similar intensity of various types of plants (e.g. grass and trees) which approximates 50% was blamed for these results. In conclusion, it was stated that the classification quality should significantly improve the inclusion of height data from laser scanning.

### 1.3 Investigation area

The study area was situated in the Widawa floodplain. The Widawa river, situated in the southern Poland (Lower Silesia), is a right-bank tributary of the Odra River. The airborne remote sensing data was collected in the strip of land along the river which was over 10 km

long and approximately 2 km wide. This strip can be divided into three sectors: the mouth sector covered with forests, the middle, agricultural sector and the upper, partly urbanized sector. The mosaic of aerial photographs of the study area covers a part of Widawa River valley in Lower Silesia, Poland. Field photographs show examples of the land cover types of the discussed floodplain.

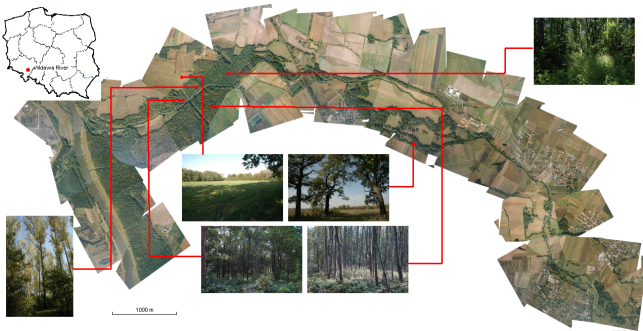


Figure 1: Mosaic of aerial photographs of the investigation area, a part of Widawa River valley in Lower Silesia, Poland. Field photographs show examples of land cover type of floodplain

## 2. FEATURE EXTRACTION

A continuous-wave (CW) ScaLars laser system was used to capture LIDAR data. On the basis of laser data, four types of information were obtained:

- differential model of height of land cover based on digital surface model (DSM) and digital terrain model (DTM),
- model of height dispersion represented by variance of measured points height in a regular grid,
- intensity image,
- model of vegetation density, the point cloud was divided using DTM into levels showing vegetation density change along vertical section in equal (1m) distance over the land surface.

As a supplementary data source aerial photographs were used. After calibration the color aerial photographs were decomposed to RGB channels. On the basis of images converted to grayscale mode, the GLCM (Gray level co-occurrence matrices) texture features were calculated. All data types were integrated with spatial resolution of 1m.

### 2.1 Aerial LIDAR height data

The experiments were carried out using information collected with ScaLARS system. This system uses Continuous-Wave (CW) laser scanner. After non-terrain points elimination using raw data, the digital terrain model and digital surface model were interpolated using the grid model. The resolution of grid was 1m. To interpolate DTM and DSM from a point cloud, a moving polynomial method was used. The differential model of height obtained on the basis of DTM and DSM is shown in the Figure 2. Generation of DSM and DTM is a time consuming process. Thus, as an alternative for height differential model, a height variance of raw laser scanning data was suggested. This feature refers to the regular, 1m grid and as a surface unit, 3m square mask was experimentally chosen. The visualization of height variance of measured points is presented in the Figure 3. Raw laser scanning data contains many survey points, which are re-

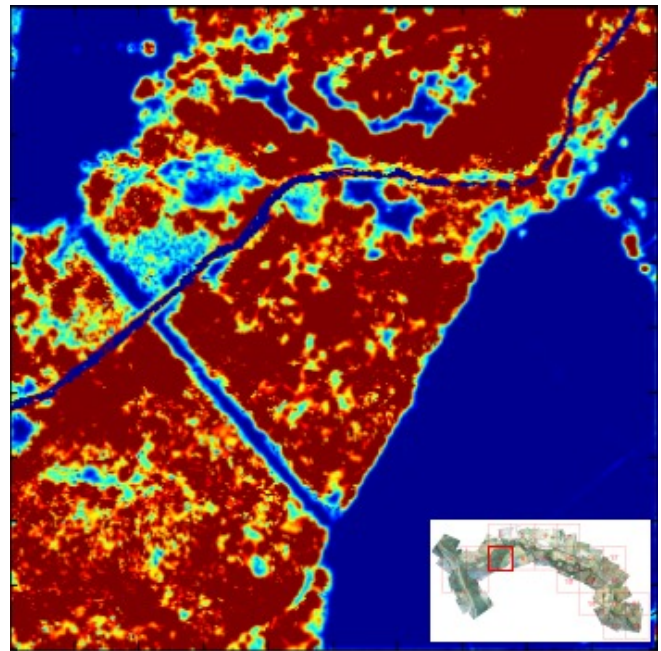


Figure 2: A part of differential model of height

flections from different types of land covers. In the wooded areas, one group of registered points is represented by points which are reflections from the surface and the other group is represented by points which are reflections from vegetation. Due to the fact that laser rays can penetrate wooden areas, tree-coverage density may be assessed on the strength of the amount of laser reflections (number of points) on particular levels over the surface. The model of vegetation density was generated by dividing the cloud point registered with a scanner with planes that occur every 1 meter. If at least one reflection was registered in a given section, it was marked with a point (1m grid). Then, on the basis of previously created DTM, plains were transformed into surfaces that were parallel to the earth surface. In this way, binary information on the reflection height was obtained. In total, 30 sections that occur every 1 meter were obtained (the maximum height of tree crowns was about 30m). The visualization of the fragment of vegetation density model is presented in the Figure 4.

### 2.2 Intensity image

In addition to geometrical coordinates, laser scanning systems also give the intensity of laser beam reflected from the surface. This feature includes some information on the land cover and can be used in classification process. However, its usefulness in afforested areas is still the subject of discussion in literature (Hofle and Pfeifer, 2007). In recent years we can observe growing interest in this field and attempts to extend its application. For instant, it was observed that for some mountainous areas, where luminance conditions are poor, the only information about texture can be laser scanning image intensity. Original intensity data has to be calibrated and interpolated into intensity image before using. In the project only coarse calibration was performed, based on a distance between the sensor and scanning point on the reflective surface (Hofle and Pfeifer, 2007):

$$I(D_s) = \frac{I \cdot D^2}{D_s} \quad (1)$$

where  $I$  is registered intensity for single point,  $D$  is a distance between sensor and measured point and  $D_s$  is a standard distance. Because large part of study area was wooded, precise calibration on satisfying level was not possible. In the Figure 5 normalized intensity image was shown for a part of investigation area. Despite

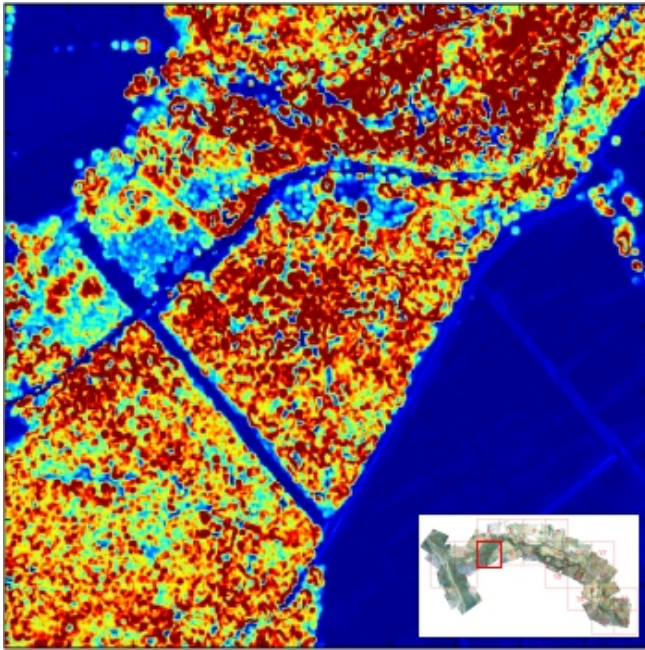


Figure 3: A part of height dispersion model

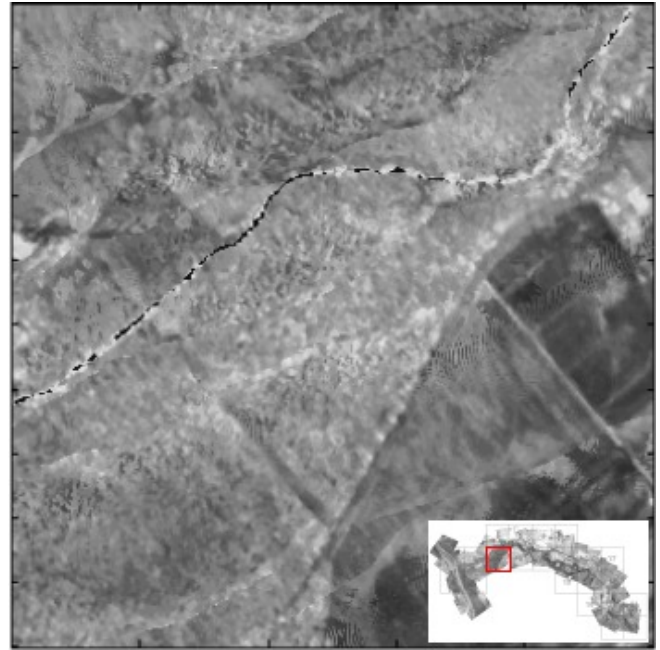


Figure 5: A part of intensity image

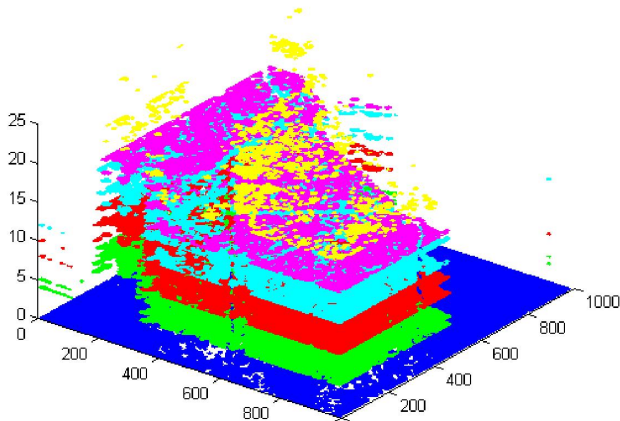


Figure 4: A part of vegetation density model

calibration drawbacks (the borders of particular scans are vivid), one can notice water and borders of afforested areas or floodbanks. Nevertheless this image was used in classification. It was assumed that it would improve identification of objects and noticeable borders between scans, which may contribute to administration of additional classes, will be classified as a noise if they coincide with other components of the feature vector.

### 2.3 Aerial images

During laser scanning data capturing, the image of the scanned area is often recorded as a video or as pictures for interpretation purposes. A number of non-metric pictures were taken with the Nikon d70W digital camera. These pictures underwent geometric correction which depended on registration of these pictures in a coordinate system using projection transformation based on Nearest Neighbour resampling method. Images were transformed with control points identified on the basis of topographic map in scale 1: 10000. On average, 10 control points were applied for a single picture. The RMS error was approximately 4m. Big errors of adjustment were caused by amateur method of taking pictures. It does not influence classification methodology but it affects its quality. In the mosaic creation process, the standard method of tone equalization was used. It was assessed that the spatial density of a pixel was 1m.

The extraction of texture features was carried out to fully use information included on the aerial pictures. The Neighbour Matrix of Grey Level Co-occurrence Matrix (GLCM) was used for this purpose. This matrix represents the statistics of occurring different-tone pixels in a fixed distance. This distance is defined as follows:

$$V_{l,\alpha}(i, j) = |\{(r, s), (t, v) : I(r, s) = i, I(t, v) = j\}| \quad (2)$$

where  $i, j = 0, \dots, N - 1$ ,  $N$  - grey levels of points in the picture,  $l, \alpha$  - distance and direction angle,  $I(x, y)$ - image pixel at position  $(x, y)$  in the picture,  $(t, v) = (r + l \cos \alpha, s + l \sin \alpha)$ . GLCM matrix must be symmetric:

$$\bar{V}_{l,\alpha} = \frac{V_{l,\alpha} + V_{l,\alpha}^T}{2}, \quad (3)$$

and normalized:

$$P_{i,j} = \frac{\bar{V}_{l,\alpha}(i, j)}{\sum_{i,j=0}^{N-1} \bar{V}_{l,\alpha}(i, j)} \quad (4)$$

The following parameters were computed on the strength of GLCM matrix:

contrast:

$$\sum_{i,j=0}^{N-1} P_{i,j}(i - j)^2 \quad (5)$$

dissimilarity:

$$\sum_{i,j=0}^{N-1} P_{i,j} |i - j| \quad (6)$$

similarity:

$$\sum_{i,j=0}^{N-1} \frac{P_{i,j}}{1 + (i - j)^2} \quad (7)$$

max  $P_{i,j}$ :

$$\text{Max}(P_{i,j}) \quad (8)$$

Angular Second Moment(ASM):

$$\sum_{i,j=0}^{N-1} P_{i,j}^2 \quad (9)$$

energy:

$$\sqrt{ASM} \quad (10)$$

entropy:

$$\sum_{i,j=0}^{N-1} P_{i,j} (-\ln P_{i,j}) \quad (11)$$

This feature both with RGB channel were included in the classification vector for each pixel.

### 3. CLASSIFICATION AND QUALITY MEASURE

#### 3.1 Classification algorithms and feature vector combinations

The classification of surface roughness involves identification of distinctive classes that correspond to different land surface types and allocation of a particular class membership to each pixel (per-pixel classification). Laser scanning data was used both as the only and supplementary source of information on the land cover. All data types were integrated and numbers of experiments were performed to find the best combination of data set. Three classification methods were tested:

- multilayer neural networks,
- maximum likelihood classifier,
- k-nearest neighbour method.

On the strength of reconnaissance, 17 classes of land cover were determined on the study area. Then, their hydraulic features were evaluated using the sample area at the size of 100x100m. These classes were found in the terrain and were used as a training data for classifiers.

#### Artificial neural networks (ANN)

The application of artificial neural networks for solving problems in remote sensing has been already well-established (Liu et al., 2002, Miller et al., 1995, German and Gahegan, 1996). The networks applied were a feed-forward, multi-layer ones trained by means of Standard Back-propagation method using hand-crafted reference data. Neural classifier consists of number of neurons combined together. The input layer size is determined by the feature vector size and the output layer is determined by the number of classes. The architecture of the hidden layer influences classification result. The topology of network which would optimally resolve classification problem was found through experiments.

#### Maximum likelihood method (MLM)

Maximum likelihood classifier combines probability model with a decision rule, which is specified as the choice of the most probable hypothesis. This rule is called maximum a posteriori rule:

$$\Psi^*(x) = j \Rightarrow p_j f_j(x) = \max_{k \in M} p_k f_k(x), \quad (12)$$

where:  $x = [x_1 \dots x_n]$  is a vector of features,  $j, k$  are labels of classes,  $p_j$  - probability, that observed case belongs to the class  $j$  (a

priori probability),  $f_j(x)$  density function. A priori probability  $p_j$  was approximated using formula:

$$\tilde{p}_j = \frac{N_j}{N}, \quad j \in M, \quad (13)$$

where:  $N_j$  is a number of objects in class  $j$  and  $N$  is a number of all objects. The density function  $f_j(x)$  was approximated by the multidimensional normal distributions:

$$f_j(x) = \frac{1}{(2\pi)^{\frac{k}{2}} |E_j|^{\frac{1}{2}}} e^{-\frac{1}{2}(x-m_j)^T E_j^{-1}(x-m_j)}, \quad (14)$$

where:  $m_j$  - mean value vector,  $E_j$  - feature covariance matrix.

#### K-nearest neighbour method (k-NN)

K-nearest neighbour method belongs to the most simple classification algorithms. An object is classified by a majority vote to the most common class amongst its k-nearest neighbours in the learning set. In this project  $k$  parameter was experimentally established as 5.

#### 3.2 Quality measure

In literature (Brivio et al., 2002) to quantify the quality of the results in an automatic manner a confusion matrix  $A = [a_{ij}]$  method is postulated. This matrix represents a statistics of points that belong to class  $j$ , which were classified as points from class  $i$ . A confusion matrix can be defined as shown in table 1 (Iwaniak et al., 2005). Elements of  $A$  matrix, describe a number of sample pixels from the

		pattern			
		1	2	...	$M$
classification	1	$a_{11}$	$a_{12}$	...	$a_{1M}$
	2	$a_{21}$	$a_{22}$	...	$a_{2M}$
	...	...	...	...	...
	$M$	$a_{M1}$	$a_{M2}$	...	$a_{MM}$

Table 1: A confusion matrix

$j$  - th class that were classified as pixels which belong to the  $i$  - th class. The following measures calculated on the basis of confusion matrix were proposed to quantify results of this experiments:

- user accuracy of class  $i$ :

$$u_i = \frac{a_{ii}}{a_{ri}}, \quad (15)$$

where:  $a_{ri} = \sum_i a_{ri}$ . (sum of  $i$ -th row entries);

- producer accuracy of class  $i$ :

$$p_i = \frac{a_{ii}}{a_{ci}}, \quad (16)$$

where:  $a_{ci} = \sum_i a_{ci}$ . (sum of  $i$ -th column entries);

- overall accuracy  $d$ :

$$d = \frac{\sum_i a_{ii}}{a_t}, \quad (17)$$

where:  $a_t = \sum_i a_{ci} = \sum_i a_{ri}$  (sum of all elements);

- Kappa coefficient:

$$\hat{\kappa} = \frac{P_o - P_e}{1 - P_e} \quad (18)$$

where:  $P_o = \frac{\sum_i a_{ii}}{a_t}$  and  $P_e = \frac{\sum_i a_{ri} a_{ci}}{a_t^2}$



Table 2: Visualisation of the most important results (Part 1)

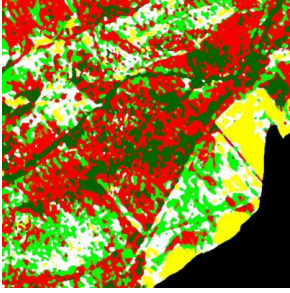
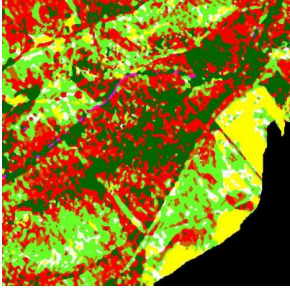
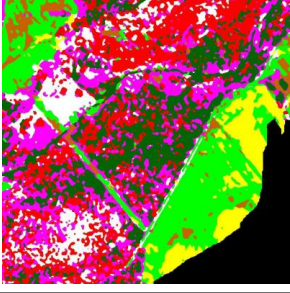
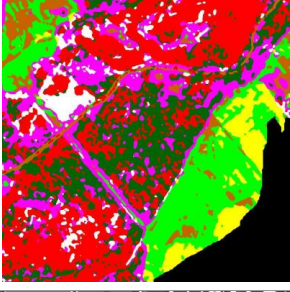
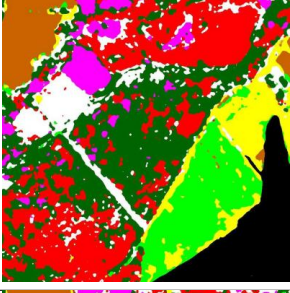
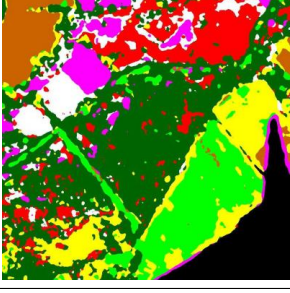
No.	Alg.	Feature vector	Visualisation
1	ANN	Intensity	
2	MLM	Intensity	
3	ANN	Intensity, Height dispersion model	
4	ANN	Intensity, Height differential model	
5	ANN	RGB, GLCM, Intensity, Height dispersion model	
6	ANN	RGB, GLCM, Intensity	

Table 3: Visualisation of the most important results (Part 2)

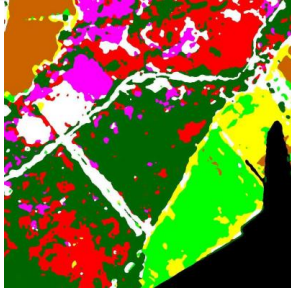
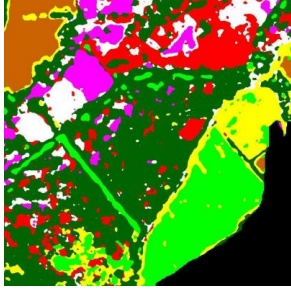
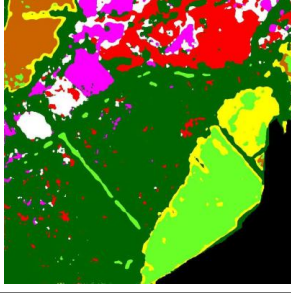
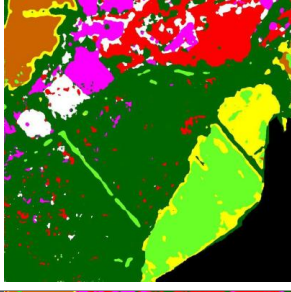
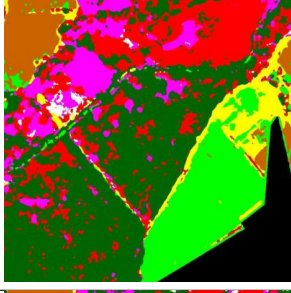
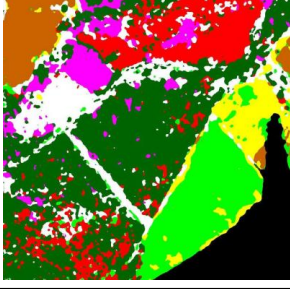
No.	Alg.	Feature vector	Visualisation
7	ANN	RGB, GLCM, Intensity, Height differential model	
8	ANN	RGB, GLCM	
9	MLM	RGB, GLCM	
10	MLM	RGB, GLCM, Intensity	
11	k-NN	RGB, GLCM, Intensity, Height differential model	
12	ANN	RGB, GLCM, Intensity, Height differential model, Model of vegetation density	

Table 4: Quality measures of the best result

Class Id	Quality measure			
	$p_i$	$u_i$	$d$	$\hat{\kappa}$
1	0.290835	0.757025	0.738917	0.670305
2	0.626177	0.644681		
3	0.498922	0.768419		
4	0.887319	0.665853		
5	0.803451	0.887200		
6	0.943158	0.920079		
7	0.648010	0.635595		
8	0.979317	0.944988		

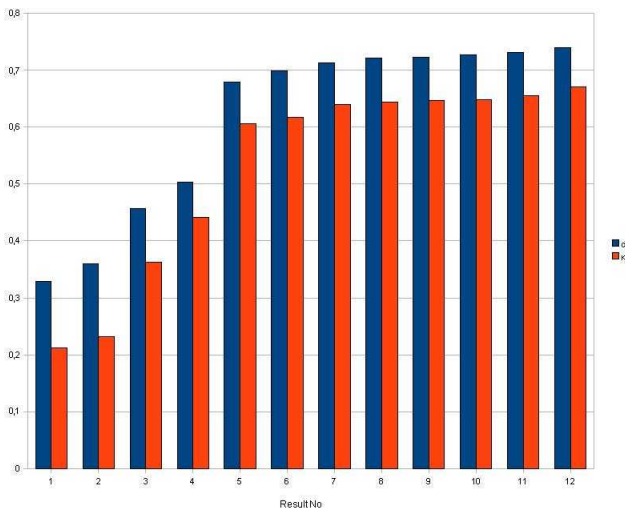


Figure 6: Quality measure comparison for the main results

#### 4. RESULTS

Tables 2 and 3 present the most important results. Qualitative, visual evaluation of conformity of the classification to the pattern shows that the best results were obtained for the method of artificial neuron networks for the feature vector that consists of RGB channels, GLCM properties, intensity and differential model of height and vegetation density model. The accuracy evaluation was made by comparison of the results with the pattern which was manually crafted. The accuracy measures for the best pattern are presented in the Table 4. Comparison of  $\hat{\kappa}$  and  $d$  coefficients for the results included in the Tables 2 and 3 is presented in the chart in the Figure 6.

#### 5. CONCLUSIONS

Experiments demonstrated that scanning data as the only source of information is insufficient for land cover classification, especially in vegetated areas. However, inclusion of height information (differential model or height variance) in classification vector along with RGB and texture features reduces errors (for example caused by the imperfection of tone equalization). Using variance of height instead of differential model estimated on the basis of DSM and DTM gives comparable results. Moreover, in comparison to DTM and DSM generation it is easy and fast to obtain this feature. Inclusion of intensity image in the feature vector does not reduce false classification rate to an appreciable degree. However, this information is useful for water detection even if it is invisible on aerial photographs. The best results are obtained by artificial neural network classifier. The maximum likelihood method usually gives similar quality, but the normal distribution model is unsuitable for height models (lack of distribution in some classes). The k-nearest neighbour method

gives unacceptable results (when taking into account visual evaluation of conformity).

#### ACKNOWLEDGEMENTS

This work was financed by Ministry Of Science and Higher Education from funds on science in 2007-2009 as a research project number N30507832/2740 and in 2005-2007 as a research project number 4T12E0172.

#### REFERENCES

- Brivio, P. A., Maggi, M., Binaghi, E., Gallo, I. and Grgoire, J.-M., 2002. Exploiting spatial and temporal information for extracting burned areas from time series of spot-vgt data. *Analysis of Multi Temporal Remote Sensing Images*. World Scientific. Singapore, pp. 133–139.
- Charaniya, A., Manduchi, R. and Lodha, S., 2004. Supervised parametric classification of aerial lidar data. Conference: Computer Vision and Pattern Recognition Workshos, pp. 30–31.
- German, G. W. H. and Gahegan, M. N., 1996. Neural network architectures for the classification of temporal image sequences. *Computers and Geosciences* 22(9), pp. 969–979.
- Hofle, B. and Pfeifer, N., 2007. Correction of laser scanning intensity data: Data and model-driven approaches. *ISPRS Journal of Photogrammetry & Remote Sensing* Vol. 62, pp. 415–433.
- Iwaniak, A., Kubik, T., Paluszynski, W. and Tymkow, P., 2005. Classification of features in high-resolution aerial photographs using neural networks. XXII International Cartographic Conference A Coruna (Spain)[CD-ROM].
- Katzenbeisser, R., 2003. TopoSys gmbh technical note, [http://www.toposys.de/pdfext/\(accessed 20 Sep. 2007\)](http://www.toposys.de/pdfext/(accessed 20 Sep. 2007)).
- Liu, X.-H., Skidmore, A. and Oosten, H. V., 2002. Integration of classification methods for improvement of land-cover map accuracy. *ISPRS Journal of Photogrammetry & Remote Sensing* 56(4), pp. 257–268.
- Miller, D. M., Kaminsky, E. J. and Rana, S., 1995. Neural network classification of remote-sensing data. *Computers and Geosciences* 21(3), pp. 377–386.
- Song, J., Han, S. and Kim, Y., 2002. Assessing the possibility of land-cover classification using lidar intensity data. *International Archives of Photogrammetry and Remote Sensing*, Graz Vol. XXXIV/3B, pp. 259–262.